Disrupted basolateral amygdala circuits supports negative valence bias in depressive states

Mathilde Bigot, Claire-Hélène de Badts, Axel Benchetrit, Éléonore Vicq, Carine Moigneu, Manon Meyrel, Sébastien Wagner, Alexandru Adrian Hennrich, Josselin Houenou, Pierre-Marie Lledo, et al.

ARTICLE OPEN

Check for updates

Disrupted basolateral amygdala circuits supports negative valence bias in depressive states

Mathilde Bigot[1,2], Claire-Hélène De Badts[1], Axel Benchetrit[1], Éléonore Vicq[1], Carine Moigneu[1], Manon Meyrel[3,4,5], Sébastien Wagner[1], Alexandru Adrian Hennrich[6], Josselin Houenou[3,4,5], Pierre-Marie Lledo[1], Chantal Henry[1,7,8,9]✉ and Mariana Alonso[1,9]✉

Negative bias is an essential characteristic of depressive episodes leading patients to attribute more negative valence to environmental cues. This negative bias affects all levels of information processing including emotional response, attention and memory, leading to the development and maintenance of depressive symptoms. In this context, pleasant stimuli become less attractive and unpleasant ones more aversive, yet the related neural circuits underlying this bias remain largely unknown. By studying a mice model for depression chronically receiving corticosterone (CORT), we showed a negative bias in valence attribution to olfactory stimuli that responds to antidepressant drug. This result paralleled the alterations in odor value assignment we observed in bipolar depressed patients. Given the crucial role of amygdala in valence coding and its strong link with depression, we hypothesized that basolateral amygdala (BLA) circuits alterations might support negative shift associated with depressive states. Contrary to humans, where limits in spatial resolution of imaging tools impair easy amygdala segmentation, recently unravelled specific BLA circuits implicated in negative and positive valence attribution could be studied in mice. Combining CTB and rabies-based tracing with ex vivo measurements of neuronal activity, we demonstrated that negative valence bias is supported by disrupted activity of specific BLA circuits during depressive states. Chronic CORT administration induced decreased recruitment of BLA-to-NAc neurons preferentially involved in positive valence encoding, while increasing recruitment of BLA-to-CeA neurons preferentially involved in negative valence encoding. Importantly, this dysfunction was dampened by chemogenetic hyperactivation of BLA-to-NAc neurons. Moreover, altered BLA activity correlated with durable presynaptic connectivity changes coming from the paraventricular nucleus of the thalamus, recently demonstrated as orchestrating valence assignment in the amygdala. Together, our findings suggest that specific BLA circuits alterations might support negative bias in depressive states and provide new avenues for translational research to understand the mechanisms underlying depression and treatment efficacy.

Translational Psychiatry (2024)14:382 ; https://doi.org/10.1038/s41398-024-03085-6

INTRODUCTION

Depression is the single largest contributor to disability worldwide, affecting 300 million people annually [1]. Depressive episodes occur in patients suffering from major depressive disorder (MDD) and bipolar disorders. Negative affective bias is an essential characteristic of depressive episodes leading patients to attribute more negative valence to environmental cues [2–5]. This negative bias affects all levels of information including perception, attention and memory linked to emotional stimuli. These biases lead to the development and maintenance of depressive symptoms and are assessed by various tests in humans [6]. However, there are very few tests in animals to measure emotional bias in a translational way [7, 8].

Theoretical models emphasize the role of decreased top-down modulation of emotion as well as increased bottom-up response to emotional stimuli, linked to the already described cortico-limbic circuit disruptions [6, 9]. Brain imaging data show an alteration in the anatomy, the activity and connectivity of limbic regions and particularly the amygdala in depressive disorders [10–15]. Especially, overactivation of the amygdala has been described in depressed subjects, and is thought of as a key player in emotional disturbances [10]. Even more, some studies found that depressed subjects display an hyperactivation for negative stimuli and hypoactivation for positive stimuli that goes in relation to a more negative appreciation of emotional stimuli [10, 16].

In most clinical studies the amygdala is analyzed as a single homogeneous structure, without considering the complexity of amygdala subnuclei organization and its involvement in emotional response to positive and negative valence cues [17]. Recent robust findings in animal studies highlighted how

[1]Institut Pasteur, Université Paris Cité, Centre National de la Recherche Scientifique, Unité Mixte de Recherche 3571, Perception and Action Unit, F-75015 Paris, France. [2]Sorbonne Université, Collège doctoral, Paris, France. [3]Assistance Publique-Hôpitaux de Paris, Department of psychiatry, Mondor University Hospital, Créteil, France. [4]NeuroSpin, PsyBrain Team, UNIACT Lab, CEA Saclay, Gif-sur-Yvette, France. [5]Université Paris Est Créteil, Faculté de Santé de Créteil, INSERM U955, IMRB, Translational Neuropsychiatry team, Créteil, France. [6]Max von Pettenkofer-Institute Virology, Medical Faculty, and Gene Center, Ludwig Maximilians University Munich, Munich, Germany. [7]Université de Paris Cité, Paris, France. [8]Departement of Psychiatry, Service Hospitalo-Universitaire, GHU Paris Psychiatrie & Neurosciences, Paris, France. [9]These authors contributed equally: Chantal Henry, Mariana Alonso. ✉email: ch.henry@ghu-paris.fr; mariana.alonso@pasteur.fr

Received: 25 July 2023 Revised: 29 August 2024 Accepted: 2 September 2024
Published online: 19 September 2024

basolateral amygdala (BLA) circuits assign positive and negative valences to emotional stimuli [18]. BLA neurons preferentially involved either in positive or negative valence coding can be distinguished according to their projection targets as well as to spatial and genetic characteristics [18]. The BLA neurons projecting to the nucleus accumbens (NAc) mainly respond to positive stimuli and trigger approach behaviors, while BLA neurons targeting the centromedial nucleus of the amygdala (CeA) mainly respond to negative stimuli, generating defensive responses, despite genetic and functional heterogeneity reported in some studies [19–24].

Many clinical and preclinical studies on negativity in depression focused on cognitive biases and disruption of cortical top-down inputs [6]. Here we propose to study how alteration in valence attribution towards emotional stimuli underly negative bias in depression. By using a translational approach, we analyzed the valence attributed to olfactory stimuli in both humans and mice. As we observed a similar olfactory negative bias in depressed patients and mouse model for depression, we explored the underlying mechanisms in animal. We hypothesized that disrupted neuronal activity of specific BLA circuits supports negative bias associated with depressive states.

METHODS AND MATERIALS

Human subjects and Sniffin' sticks test

The Human Research Ethics Committee, CPP-Ile de France IV (2015/44), approved the study and all participants gave their informed consent. Forty-eight patients were included in our study, aged from 18 to 65 years, with a current bipolar disorder diagnosis (BP I ($n = 29$) and BP II ($n = 18$)) according to the DSM-IV criteria [25], and 11 control subjects. Among the recruited patients, 25 subjects presented an euthymic state and 23 a depressive or mixed state at the moment of the evaluation. There were no differences between the groups in terms of gender, age or level of education. Depression severity was measured by MADRS scale and manic symptoms by YMRS scale (for more details see table S1). All euthymic and depressive patients were on a mood stabilizer.

Odor valence assignment was evaluated during the identification task of the Sniffin' sticks test (Burghardt®, Germany), as previously published [26] (see also Supplemental information for more details).

Animals and chronic corticosterone administration model for depression

All animal care and experimental procedures followed national and European (2010/63/EU) guidelines and were approved by the French Ministry of Research (APAFiS: #16380-2018080217358599_v1). C57BL/6 N male mice (7–8 weeks old, Taconic Farms (Denmark), $n = 181$) were socially housed (4–6 per cage) and maintained under standard conditions (23 ± 1 °C; humidity 40%) on a 14/10 h light/dark cycle with food and water *ad libitum*.

Corticosterone (CORT, 35 µg/ml, equivalent to about 5 mg/kg/day) was prepared in vehicle made of 0.45% (2-hydroxypropyl)-beta-cyclodextrin (β-CD; both from Sigma-Aldrich, France), and administered in drinking water for 28 days, as previously described [27]. After four weeks of CORT treatment, the fluoxetine hydrochloride antidepressant (equivalent to about 18 mg/kg/day; Sigma-Aldrich) was administered for three weeks along with CORT administration [27].

Behavioral assessment

Several behavioral tests assessed anxiety, depression-like phenotypes, and olfactory preferences. The olfactory preference test was performed in a quiet and dimly lit room (adapted from [28]). Clean housing cages with regular bedding material were used as testing arenas. A petri dish with hooled cover was placed at one side of the arena. The behavior was recorded by video camera for 15 min and the Noldus Ethovision 11.0 (Netherlands) system was used to track position and locomotion of mice. During the first 4 days, only a Whatman paper filter (GE Healthcare Life Sciences, USA) was placed into the petri dish, to assess baseline exploration. Then, 2 days were dedicated to each odor with the odorant placed on paper filter in the following order: peanut oil (pure, 400 ul), female urine (pure, 100 ul), trimethylamine (Sigma-Aldrich, 6.75% in water, 400 ul) and trimethylthiazoline (Sigma-Aldrich, 5% in mineral oil, 400 ul) (see Supplemental information for more details).

CTB stereotaxic injections

To label neurons of the BLA projecting to NAc or CeA, the retrograde tracer Cholera Toxin Subunit B conjugated with Alexa Fluor 555 or 674 (CTB 555 or CTB 647, 1 mg/ml, Invitrogen, USA) was bilaterally injected with a micropipette connected to Nanoject III microinjector (Drummond Scientific) in the NAc (AP : +1.4 mm ; ML : ±0.87 mm ; DV : −4.35 mm, 300 nl) or in the CeA (AP : −0.8 mm, ML : ±2.35 mm, DV : −4.35 mm, 100 nl, targeting the centromedial part).

Viral stereotaxic injections

For labelling presynaptic inputs to BLA-to-NAc and BLA-to-CeA neurons, AAV-FLEX-G-TVA-GFP was injected bilaterally in the BLA (AP: −1.75 mm, ML: ±3.15 mm, DV: −4.25 mm, 100 nl) and AAVretro-CRE either in the NAc (100 nl) or in the CeA (50 nl) using previously mentioned coordinates. After four weeks of CORT treatment, mice were injected with EnvA-RVΔG-mCherry (150 nl) in the BLA and sacrificed one week later.

AAV5-hSyn-DIO-hM3Dq-mCherry, AAV5-hSyn-DIO-mCherry and AAVretro-PGK-Cre recombinant adeno-associated virus were used to manipulate BLA neuronal activity. Viral vectors were bilaterally injected into the BLA (100–150 nl) and the NAc (100–150 nl) or the CeA (50 nl) using previously mentioned coordinates.

All AAV were provided by Addgene (USA) and EnvA-RVΔG-mCherry was generated by Karl-Klaus Conzelmann lab (University of Munich, Germany).

Immunohistochemistry and image analysis

Mice were anesthetized with ketamine/xylazine mix (intraperitoneal (i.p)., 100-125 mg/kg and 50 mg/kg respectively) and perfused transcardially with 0.9% NaCl, followed by 4% paraformaldehyde in phosphate buffer, pH 7.3. Forty-micrometer-thick coronal brain sections were obtained using a sliding microtome (Leica SM 2010 R). Immunostaining was performed on free-floating sections using the following antibodies: guinea pig anti-c-Fos (1:2000, Synaptic Systems, Germany), rabbit anti-RFP (1:4000, Rockland, USA), chicken anti-GFP (1:1000, Abcam), mouse anti-CamkII (1:500, Abcam) and secondary antibodies (Alexa-conjugated secondary antibodies at 1:1000, Jackson ImmunoResearch Laboratories, United Kindom and Molecular Probes, USA).

Statistical analysis

Statistical analyses were performed with GraphPad Prism v9 software (USA). Two-sided parametric or non-parametric tests were used according to the normality of datasets and variances homoscedasticity. Following post-hoc analyses were applied with the False Rate Discovery (FDR) correction method.

All datasets were described using the mean; error bars in the figures represent standard error mean (SEM), except for Figure S4E–G where box-and-whiskers plots were used (boxes represent the 25th, median and 75th percentiles while whiskers represent the 1st and 99th percentiles). Differences were considered statistically significant for $p < 0.05$.

Detailed methods and materials can be found in the Supplemental information.

RESULTS

Negative olfactory valence bias in human patients and CORT-induced mouse model for depression

We evaluated odor valence assigment in a cohort of bipolar patients compared to control subjects using the Sniffin' sticks test [26, 29, 30]. Patients were classified based on the DSM-IV-R [25] as in remitted, and depressed or mixed state (referred to collectively as "depressed bipolar patients"). Further demographic, clinical and olfactory performance characteristics are presented in Supplementary Table 1.

Depressed bipolar patients rated less odors as pleasant than remitted bipolar patients, and more odors as unpleasant than both control subjects and remitted bipolar patients (Fig. 1A). This negative olfactory valence bias was associated with depression severity, as the MADRS score correlated negatively with the

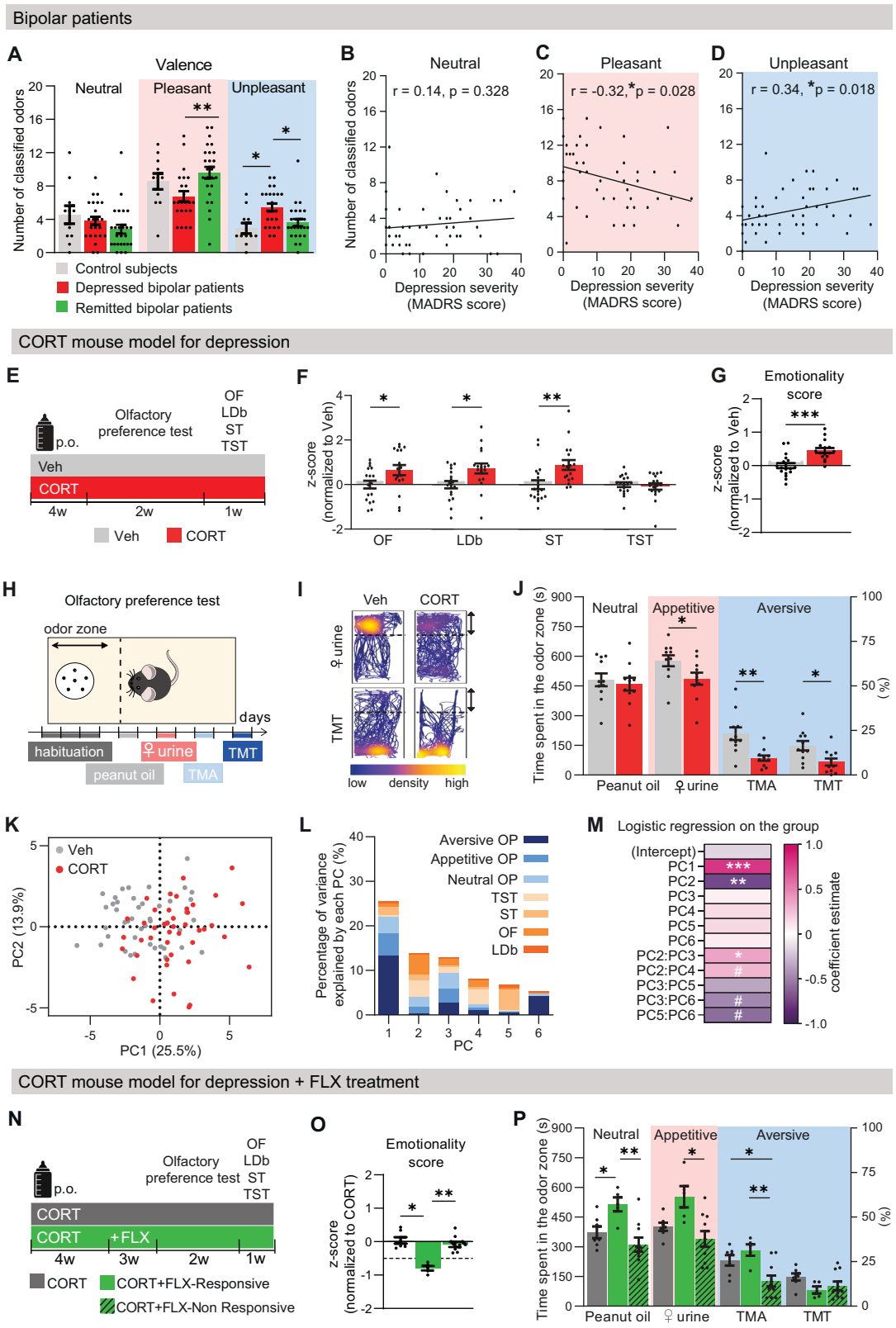

number of classified pleasant odors, and positively with the number of classified unpleasant odors in bipolar patients (Fig. 1C, D). No correlation was found between the number of classified neutral odors and depression severity (Fig. 1B). Importantly, both remitted 'euthymic' and depressive bipolar patients were treated with mood stabilizer, suggesting that the negative bias was linked to depressive state, independently of medication.

Then, olfactory valence was evaluated in mouse model for depression. We chose the well-described mouse model for depression induced by four weeks of CORT administration in drinking water [27] (Fig. 1E and Fig. S1A, B). We confirmed the

Fig. 1 Negative olfactory valence bias in depressed patients and CORT-model of depression in mice. A Depressed bipolar patients ($n = 23$) classified less odors as pleasant ones than control subjects ($n = 11$) and remitted bipolar patients ($n = 25$; $^{**}p < 0.01$), and more as unpleasant ones compared to remitted bipolar depresssed patients and control subjects ($^{*}p < 0.05$) (Group: $F(2,56) = 0.00$, $p > 0.999$, Valence: $F(2,112) = 30.1$, $p < 0.001$, Interaction: $F(4,112) = 4.15$, $p = 0.004$). **B**–**D** The number of classified neutral odors did not change with depression severity (**B**). Bipolar depressive patients with higher depression severity (i.e. higher MADRS score) classified less odors as pleasant (**C**), and more odors as unpleasant (**D**). **E** Mice received vehicle (grey, $n = 18$) or chronic CORT (red, $n = 17$) to model depression. **F** CORT mice presented anxiety-like phenotypes in the open field (OF, $t(33) = 2.26$, $p = 0.030$) and light and dark box (LDb, $t(33) = 2.62$, $p = 0.013$), and depressive-like behaviors in the splash test (ST, $U = 59$, $p = 0.001$) but not in the tail suspension test (TST, $U = 149$, $p = 0.909$). **G** Global emotionality score is increased in CORT mice ($t(32) = 4.23$). **H** Scheme of the olfactory preference test using neutral (grey), appetitive (pink) and aversive (blue) odors. **I** Representative mouse tracks colored by the density of position points. **J** CORT mice explored less ♀ urine, TMA and TMT than Veh controls (Group: $F(1,20) = 10.63$, $p = 0.004$; Odor: $F(3.60) = 163.50$, $p < 0.001$; Interaction: $F(3.60) = 1.54$, $p = 0.214$). **K** Principal Component Analysis on the 23 behavioral parameters evaluated in 87 mice from both CORT (red) and Veh (grey) mice. **L** The olfactory preference test (OP) standed for 86% of contributions to PC1 (blue bar parts). The OF (32%) and TST (28%) contributed mostly to PC2. **M** PC1, PC2 and PC2:PC3 significantly predicted the Veh/CORT status. **N** Mice received chronic CORT to model depression (grey, $n = 7$), or CORT for 4 weeks then fluoxetine in addition to CORT for the following weeks (green, $n = 14$). **O** The reduction of the global emotionality score shows an improvement of the depressed- and anxious-like phenotype in responsive mice ($U = 11.78$, $p = 0.0005$). Fluoxetine-responsive mice are defined by an emotionality score lower than -0.5. **P** CORT + FLX-Responsive ($n = 5$) mice explored more peanut oil and ♀ urine, but less TMA, than CORT ($n = 7$) and CORT + FLX-Non Responsive ($n = 9$) groups (Group: $F(2,19) = 9.629$, $p = 0.0013$; Odor: $F(2.192) = 86.61$, $p < 0.001$; Interaction: $F(6.57) = 4.11$, $p = 0.0017$). $^{\#}0.05 \leq p < 0.1$, $^{*}p < 0.05$, $^{**}p < 0.01$, $^{***}p < 0.001$. Bars are mean ± sem.

anxiety-like phenotype in the open field (OF) and light and dark box (LDb) (Fig. 1F and S1D–H), and the depressive-like behavior in the splash test (ST) (Fig. 1F and Fig. S1I–K; z-scores calculated with the different parameters recorded for each behavioral test, as described in Supplementary information). As previously reported, CORT-treated mice did not express despair-like features in the tail suspension test (TST) [31] (Fig. 1F and Fig. S1L–N). By computing an emotionality score we can globally characterize animal effective state in our model beyond single behavior test measurement (see Supplementary information). Overall, global emotionality score was significantly increased in CORT mice confirming an anxiety and depressive-like phenotype (Fig. 1G).

To assess valence assignment in mice, we set up an olfactory preference test (Fig. 1H). Each odor was presented on two consecutive days, and its attributed valence was defined by increased, decreased or similar odor zone exploration time compared to habituation in Vehicle (Veh)-treated control mice (One-way repeated measures (RM) ANOVA: $F(4,40) = 44.86$, $p < 0.001$, followed by FDR post-hoc comparisons). Peanut oil was neutral in our experimental conditions ($t(40) = 1.36$, $q = 0.183$), whereas female urine was appetitive ($t(40) = 3.85$, $q < 0.001$) and synthetic compounds trimethylamine (TMA) and 2,4,5-trimethylthiazole (TMT) were aversive (TMA: $t(40) = 5.68$, $q < 0.001$, TMT: $t(40) = 7.27$, $q < 0.001$).

CORT-treated mice investigated both appetitive female urine and aversive TMA and TMT in a lesser extent than Veh-treated controls, as revealed by decreased exploration time of the odor zone (Fig. 1I, J), reduced distance moved (Fig. S1P) and farther mean location to the odor zone (Fig. S1Q). This negative olfactory valence bias was specific for non-neutral odors, without differences in the peanut oil exploration (Fig. 1J), or during habituation (Fig. S1O).

We wondered if this olfactory valence bias distinguishing CORT-treated mice from Veh-treated controls revealed behavioral variability already measured by other behavioral tests, or could be considered as new behavioral feature. Therefore, we applied principal component analysis (PCA) on a set of data containing 87 mice (44 Veh and 43 CORT) evaluated with all the tests presented in Fig. 1F, i.e. through 23 behavioral parameters (Fig. 1K). We selected the six first PCs, representing 72.6% of explained variance. Among each PC, we summed for each test the contribution of the different recorded behavioral parameters (Fig. 1L), so that the neutral, appetitive and aversive parts of the olfactory preference test (OP) contributed respectively to 15%, 20% and 51% to the PC1, 27%, 24% and 21% to PC3, and 7%, < 1% and 78% to PC6. Contributions to PC2 were mainly driven by the OF (32%) and the TST (28%). The TST was also the major contributor to PC4 (40%). The ST contributed to 7% of PC1 and 8% of PC2, but 68% of PC5, and the LDb contributed to 13% of PC5. The relative segregation of olfactory preference test measurements from other tests in the PC1, PC3 and PC6 suggested that these olfactory parameters did not correlate with the LDb, OF, ST and TST, but rather captured variability on another dimension. We then performed a logistic regression on the group (Veh/CORT status) using the PCs and their second order interactions as predictors. AIC-based stepwise regression allowed us to select the minimal number of predictors while keeping the most information (Supplementary information, Fig. 1M). Predictors significantly associated with the group were PC1, PC2 and the interaction PC2:PC3, whereas PC2:PC4, PC3:PC6 and PC5:PC6 showed a statistical trend to association with the group.

Finally, we verified if negative olfactory valence bias observed in depressive-like mice was sensitive to antidepressant administration, as we observed in remitted bipolar patients after pharmacological treatment (Fig. 1A). After four weeks of CORT administration, mice were treated with Fluoxetine (FLX) in drinking water for three additional weeks. We compared FLX-treated animals with mice administered with CORT alone in the different behavioral tests previously used (Fig. 1N and Fig. S2). In agreement with previous data [32], FLX-treated group showed significally reduced emotionality score compared to CORT group indicating reduced anxiety and depression levels, even though this group was extremely heterogeneous (Fig. S2D). Clinical response to antidepressants in depression is defined as 50% decrease in rating scale score [33]. Thus, we analyzed our behavioral data according to this 50% cut-off, as previously described [32]. We defined FLX responsive mice with the criterion of global emotionality score under -0.5 (CORT + FLX-Responsive) where mice with emotionality score above -0.5 were defined as non-responsive (CORT + FLX-Non Responsive; Fig. 1O). CORT + FLX-Responsive mice showed an increased exploration time for neutral and appetitive odors compared to CORT and CORT-FLX-Non Responsive mice (Fig. 1P; Fig. S2S), and their mean position was closer to the odor zone for these stimuli (Fig. S2R). Surprinsingly, TMA was more repulsive for CORT-FLX-Non Responsive mice, while there was no difference in TMT exploration compared to CORT mice (Fig. 1P and Fig. S2R, S). No effect was observed during habituation or for distance moved (Fig. S2P, Q).

In summary, these results suggest that olfactory valence assignment is an independent and suitable behavioral measurement to predict differences between control and depressive-like states in mice, paralleling humans patients findings. Importantly, relief of depressive state in remitted patients and responsive mice was associated with partial improvement of negative olfacory valence bias.

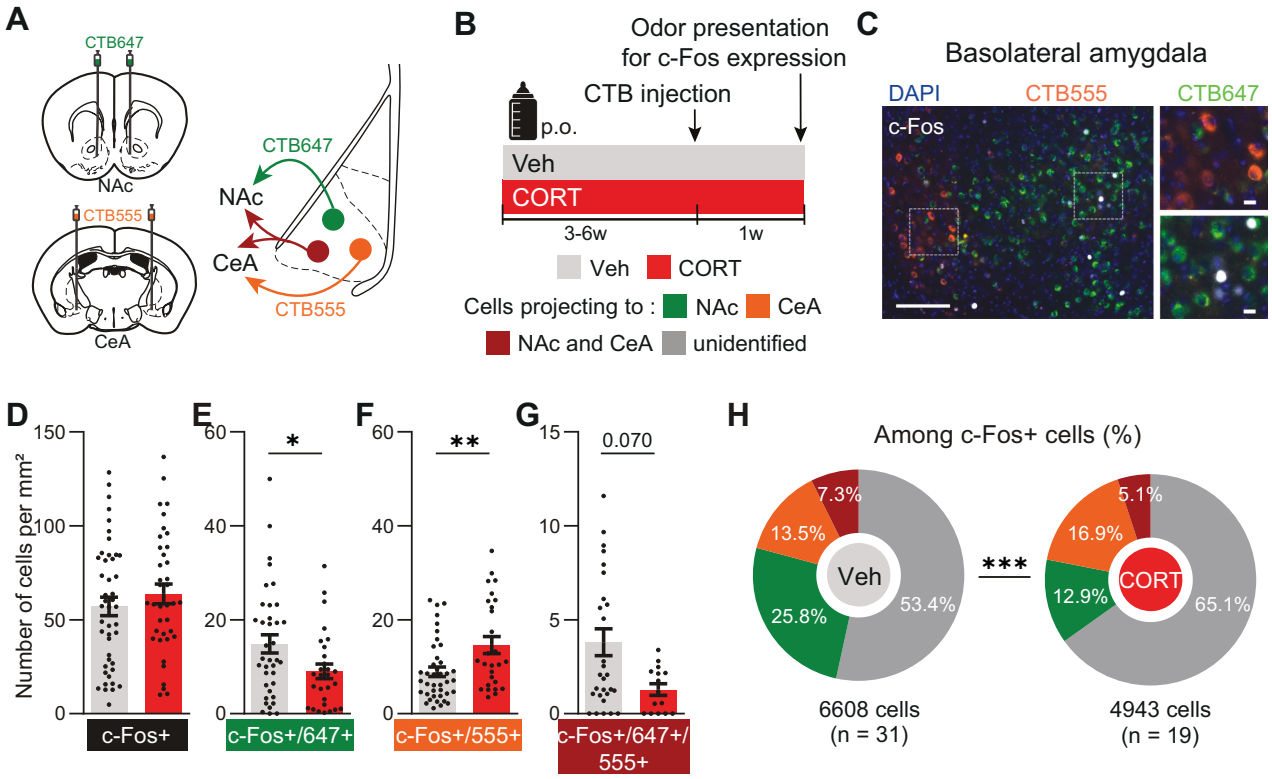

Fig. 2 Altered BLA circuits activity after chronic CORT administration. A, B Retrograde fluorescent CTB647 and CTB555 dyes were injected in the NAc (green) and CeA (orange) respectively. Odors were presented to trigger the immediate-early gene c-Fos expression in CORT (red) and Veh (grey) mice. **C** Representative image of BLA c-Fos expression colocalized with CTB647 and/or CTB555. Scale bars, 100 µm (left) and 20 µm (right). **D–H** Quantification of c-Fos+ (**D**), c-Fos + /CTB647 + **E**), c-Fos + /CTB555+ (**F**) and c-Fos + /CTB647 + /CTB555+ cell number (**G**) in the BLA. BLA c-Fos+ cell density was similar between groups (**D**, t[81] = 0.93, $p = 0.356$, Veh $n = 45$; CORT $n = 38$). BLA c-Fos + /CTB647+ cell density decreased in CORT mice (**E**, U = 356, $^{*}p = 0.032$, Veh $n = 37$, CORT $n = 28$), whereas c-Fos + /CTB555+ cell density increased (**F**, U = 328, $^{**}p = 0.006$, Veh $n = 40$, CORT $n = 27$). BLA c-Fos + /CTB647 + /CTB555+ cell density tended to decrease in CORT mice (**G**, U = 144.5, $p = 0.070$, Veh $n = 29$, CORT $n = 15$) (**H**) Distribution of CTB647 and/or CTB555 colocalization among the total number of c-Fos+ cells in the BLA ($\chi^2(3) = 340.0$, $^{***}p < 0.001$). Bars are mean ± sem.

BLA circuits activity alterations in CORT-induced mouse model for depression

According to the major role of BLA in valence processing, we hypothesized that activity of BLA-to-NAc projecting neurons would be reduced in depressive states while BLA-to-CeA neurons would be more active. Thus, we injected retrograde CTB647 and CTB555 dyes in the NAc and CeA respectively (Fig. 2A and Fig. S3) to label BLA projecting neurons to these structures. Injections were performed in both CORT or Veh-treated mice, one week before presenting odors to trigger c-Fos expression, used as immunohistological proxy for neuronal activation (as we previously performed [34]; Fig. 2B, C). We used Icy software to automatically detect c-Fos +, colocalizing c-Fos + /CTB647 +, c-Fos + /CTB555+ and c-Fos + /CTB647 + /CTB555+ cells (Fig. S4D–G, Supplementary information). Although odorless mineral oil, appetitive female urine and aversive TMT recruited different proportion of the BLA-to-NAc, BLA-to-CeA and BLA-to-NAc-and-CeA neurons both in Veh-treated control and in CORT-treated mice, the total density of c-Fos+ and colocalizing c-Fos + /CTB+ cells were mostly similar across odors and groups (Fig. S4H–J and Table S2) and the total c-Fos+ cell number did not differ between Veh and CORT-treated groups in the BLA (Fig. 2D). Importantly, no differences were found between groups in the density of both CTB647+ and CTB555+ cells (Fig. S4D). When compared regardless of the odor used for c-Fos stimulation, BLA-to-NAc neurons were less active in CORT-treated mice compared to Veh-treated controls, while BLA-to-CeA neurons more active (Fig. 2E, F). BLA cells projecting to both NAc and CeA tended to be less recruited in CORT-treated mice than in Veh-treated controls (Fig. 2G). Among all BLA c-Fos+ cells, the numbers of projecting neurons were differently distributed between groups, with less BLA-to-NAc c-Fos+ cells, and more BLA-to-CeA and unidentified c-Fos+ cells in the CORT-treated mice relative to Veh-treated group (Fig. 2H).

Previous reports demonstrated specific patterns of connection and functions associated with the basal and lateral amygdala subregions (BLA or BA and LA, respectively [35–37]. However, valence coding has been inconsistently studied across these regions, analyzing either the basal part exclusively [38], or both basal and lateral parts together [20]. To study specificities of each region, we performed similar analyses in the LA showing some variations compared to (basal) BLA data. No difference was found on both LA-to-NAc and LA-to-CeA neuronal activation between Veh-treated controls and CORT-treated mice while the LA-to-NAc-and-CeA cells were more recruited in CORT-treated mice (Fig. S5 and Table S3).

In summary, chronic CORT administration induced decreased recruitment of BLA-to-NAc neurons and increased recruitment of BLA-to-CeA neurons, circuits already implicated in opposite valence encoding.

Specific alterations in presynaptic connectivity of BLA projecting neurons induced by CORT treatment

The amygdala activity is regulated by numerous afferents [39]. To understand if disruption of BLA circuits activity in CORT-treated mice could be linked with durable anatomical changes in brain

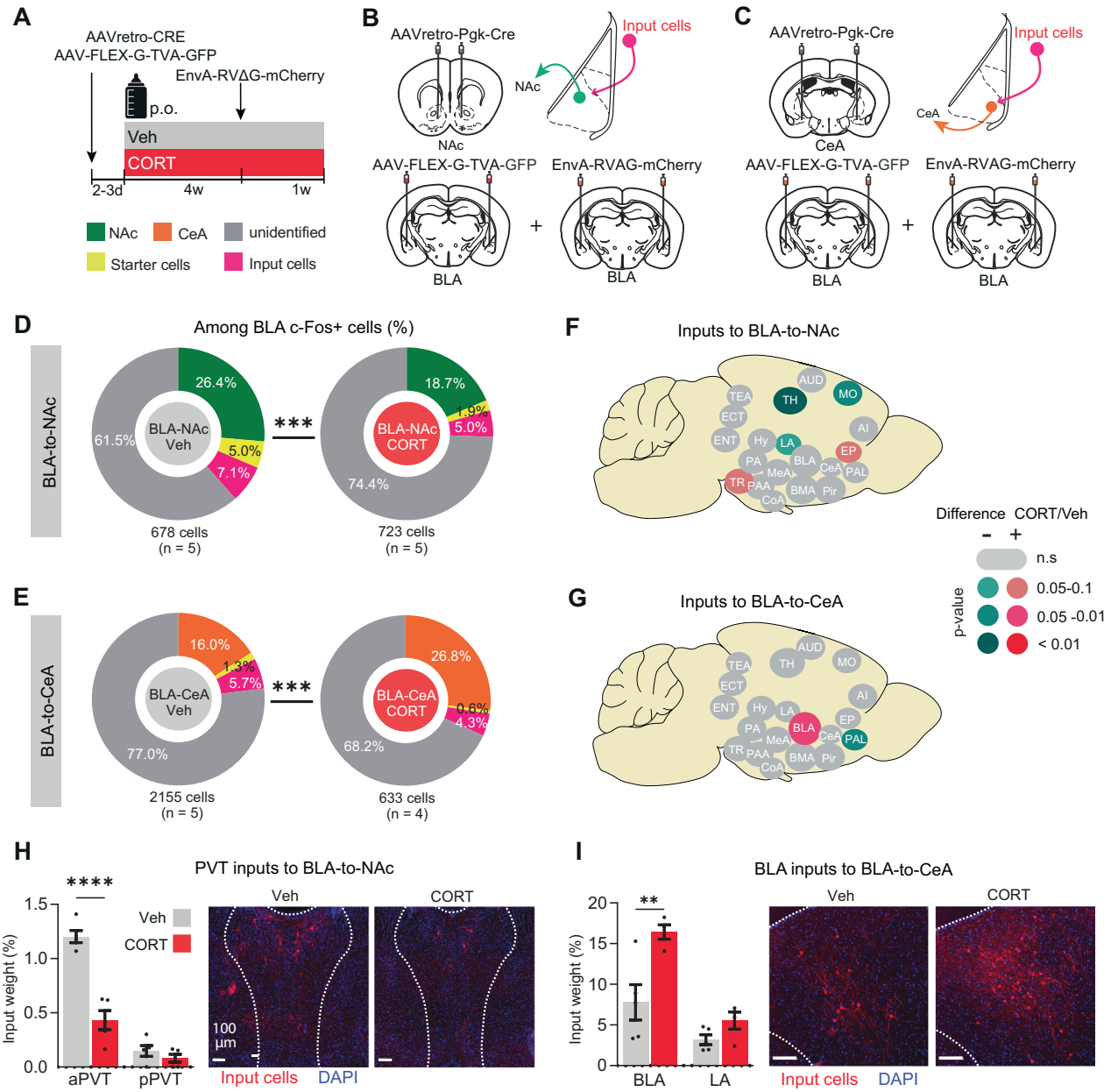

Fig. 3 CORT treatment changes synaptic connectivity of BLA neurons. A Mice received vehicle (grey, $n = 10$) or chronic CORT (red, $n = 9$) to model depression. **B** AAVr-Pgk-Cre in the NAc and AAV-hSyn-Flex-G-TVA-GFP and EnvA-RVAG-mCherryin the BLA were injected to trace monosynaptic input to BLA-to-NAc projecting cells (in green, $n = 10$). **C** Same than A except that AAVr-Pgk-Cre were injected in the CeA to labelled BLA-to-CeA cells (in orange, $n = 9$). **D, E** Distribution of BLA-to-NAc (**D**, in green) or BLA-to-CeA (**E**, in orange), starters cells (in yellow), inputs cells (in pink) and unidentifed cells (in gray) among the total number of c-Fos+ cells in the BLA (**D**: $\chi^2(3) = 35.09$, $p < 0.0001$; **E**: $\chi^2(3) = 39.58$, $p < 0.0001$). **F, G** Map of the differences in inputs arriving to BLA-to-NAc (**F**) and BLA-to-CeA (**G**) projecting neurons in CORT-treated compared to Vehicle group. Only regions showing a tendency or significant difference are colour-coded (for full data see Fig. S6H, I). **H–I** Representative images (right) and percentage of inputs neurons (left) to BLA-to-NAc (**H**) and BLA-to-CeA (**I**) arriving from subregions of PVT posterior/anterior or BLA/LA respectively, in both CORT and Veh groups (relative to the total) (**H**, BLA-to-NAc: Group: $F(1, 8) = 37.69$, $p = 0.0003$; Region: $F(1, 8) = 185.5$, $p < 0,0001$; Interaction: $F([1, 8) = 37.69$; $p = 0.0003$; (**I**), BLA-to-CeA: Group: $F(1, 7) = 12.08$, $p = 0.0103$; Region: $F([1, 7) = 39.03$, $p = 0,0004$; Interaction: $F(1, 7) = 6.489$, $p = 0.0382$). Scale bar = 100 µm (**H**) and 20 µm (**I**). MO somatomotor areas, AUD auditory areas, AI agranular insular area, TEA temporal association areas, ECT ectorhinal area, PIR piriform area, COA cortical amygdalar area, PAA piriform-amygdalar area, TR postpiriform transition area, LA lateral amygdala, BLA basolateral amygdala, BMA basomedial amygdala, PA posterior amygdala, EP endopiriform nucleus, ENT retrohippocampal region, MEA medial amygdala, CEA Central amygdala, PAL pallidum, TH thalamus; HY hypothalamus. Bars are mean ± sem.

circuits, we investigated presynaptic connectivity of the BLA projecting neurons using targeted retrograde rabies virus-based monosynaptic tracing. We restricted the rabies infection only to BLA-to-NAc or BLA-to-CeA neurons with retrograde Cre-expressing virus injected either in the NAc or the CeA, together with a conditional Cre-dependent 'helper' virus to express the avian tumor virus receptor A (TVA) and the rabies glycoprotein injected in the BLA (Fig. 3A–C). Injected animals were treated either with CORT or Veh (Fig. 3A and Fig. S6A-D). Four weeks later, we injected a glycoprotein-deleted EnvA-pseudotyped mCherry-expressing

rabies virus [(EnvA)SAD-ΔG-mCherry] that only infected neurons expressing TVA receptors and spread retrogradely only from cells expressing the glycoprotein, meaning specifically in presynaptic inputs of BLA-to-NAc or BLA-to-CeA neurons. Six days post-injection, we examined sections of the entire brain to quantify the location and the relative number of inputs neurons (mCherry +) (Fig. S6E). Labelled brain regions directly projecting onto BLA-to-NAc and BLA-to-CeA neurons were similar to those previously reported [40, 41] (Fig. S6H, I). Comparing CORT with Veh-treated mice, we established a brain map of differential contributions of input regions, revealing which brain circuits exhibited distinct connectivity patterns after depressive state induction (Fig. 3F, G and Fig. S6H, I). We observed that the thalamus region (TH) and the somatomotor areas (MO) contained fewer inputs neurons to the BLA-to-NAc neurons in the CORT-treated mice (Fig. 3F). Besides, we found more cells contacting BLA-to-CeA projecting neurons in the BLA circuit but a reduced the number in the pallidum (PAL; Fig. 3G).

More than 60% of the connections arriving from the TH originated in the paraventricular nucleus of the thalamus (PVT) (BLA-to-NAc: 67,19% ± 3,98; BLA-to-CeA: 64,11% ± 10,58, $n = 4$-5). An important proportion of these neurons expressed CaMKIIα protein, a marker for long-range glutamatergic input (BLA-to-NAc: 32.2% +/−3.95; BLA-to-CeA: 46.8% +/− 6.57; total cells analysed 202 and 94 respectively). Remarkably, CORT administration specifically reduced the number of neuronal inputs to the BLA-to-NAc neurons from the anterior PVT (aPVT) without changes from the posterior part (pPVT; Fig. 3H). Moreover, no significant differences were observed on both anterior or posterior PVT inputs to BLA-to-CeA neurons (group: F (1, 7) = 2,279 P = 0,1748, $n = 4$-5). Interestingly, CORT administration specifically increases the percentage of neuronal inputs to the BLA-to-CeA from the BLA circuit itself (Fig. 3I). Half of these local inputs arrive from CamkII+ cells impinging both BLA-to-NAc (53.3% +/− 4.07; $n = 298$ cells) and BLA-to-CeA (51.8% +/− 5.10; $n = 108$ cells) neuronal populations.

We also quantified in this experiment the activity of BLA circuits in Veh and CORT-treated mice using c-Fos staining. We replicate with a different method the observation of reduced activation of BLA-to-NAc neurons in CORT-treated mice, while stronger activity of BLA-to-CeA neurons (Fig. 3D, E, see Fig. 2H). Importantly, no significant differences were found in the total BLA c-Fos+ cell density between Veh and CORT-treated animals in both BLA-to-CeA and BLA-to-NAc groups (Fig. S6F) in agreement with data shown in Fig. 2D.

Overall, differential activation of BLA-to-NAc and BLA-to-CeA neurons after chronic CORT administration matches with significant altererations in presynaptic connectivity from the PVT, a brain region already implicated in stimuli salience [42] and valence assignment regulation [21, 43], but also with changes from local BLA inputs.

No effect of BLA-to-CeA neuronal activation on olfactory valence in control mice

To know if BLA circuits alterations had a causal role in the CORT-treated mice phenotype, we first attempted to elicit anxiety- and depressive-like behaviors as well as negative olfactory valence bias by chemogenetically activating BLA-to-CeA neurons in control mice. We injected retrograde AAVr-Pgk-Cre viral vector in the CeA and AAV-hSyn-DIO-hM3Dq-mCherry (or AVV-hSyn-DIO-mCherry) in the BLA to express hM3Dq, an activator designer receptor exclusively activated by designer drugs (DREADD), coupled with mCherry protein (or mCherry alone) specifically into BLA-to-CeA neurons (Fig. 4A). Intraperitoneal (i.p.) clozapine-n-oxide (CNO) injection was performed to activate the cells (Fig. 4B). Remarkably, chemogenetic BLA-to-CeA activation was not sufficient to trigger anxiety-like phenotypes in the OF and LDb, nor depressive-like phenotypes in the ST and TST (Fig. S7C–M), as reflected by the unchanged global emotionality score (Fig. 4C). Consistenly, it also failed to induce negative olfactory valence bias in the olfactory preference test (Fig. 4D, E and Fig. S7N–P). Importanlty, the activation of BLA-to-CeA neurons was confirmed by increased c-Fos expression (Fig. 4F, G).

Dampened negative bias after BLA-to-NAc neuronal activation in CORT mice

Secondly, we chemogenetically activated BLA-to-NAc neurons in CORT-treated mice in order to alleviate anxiety- and depressive-like phenotype, as well as the negative olfactory valence bias. We injected retrograde AAVr-Pgk-Cre viral vector in the NAc and AAV-hSyn-DIO-hM3Dq-mCherry (or AVV-hSyn-DIO-mCherry) in the BLA, to express hM3Dq coupled with mCherry protein (or mCherry alone) specifically into BLA-to-NAc neurons (Fig. 4H). We administered CORT to all animals for four weeks and then performed behavioral testing after CNO i.p. injection (Fig. 4I). Chemogenetic BLA-to-NAc neuronal activation was sufficient to improve anxiety-like behavior in CORT-hM3Dq mice compared to CORT-mCherry control mice in the OF but not in the LDb (Fig. S8D–H). It had no effect on the depressive-like phenotype measured by the ST, but had antidepressant effect on the TST (Fig. S8I–N). Overall, activating BLA-to-NAc neurons improved the global emotionality score (Fig. 4J). Strikingly, BLA-to-NAc activation also increased exploration of peanut oil and female urine in CORT-hM3Dq mice relative to CORT-mCherry controls, while leaving unchanged the aversive odors exploration (Fig. 4K, L and Fig. S8Q, R). It is worth noting that the time spent exploring the object during habituation also tended to be increased in CORT-hM3Dq mice (Fig. S8P). Once again CNO injection significativly increases the activity of BLA-to-Nac neurons as reflected by c-Fos staining (Fig. 4M, N), Therefore, BLA-to-NAc neuronal activation is sufficient to improve negative olfactory bias and potentiates positive valence assignment of neutral or appetitive odors in a mouse model for depression.

DISCUSSION

By using a translational olfactory preference test, we demonstrate for the first time that negative bias toward emotional stimuli is present for both positive and negative cues in a mouse model for depression similarly to bipolar depressed patients. Both human and mouse experiments demonstrated a spontaneous and global shift towards more negative valence assignment of both pleasant/attractive and unpleasant/aversive odors during depressive states. Depressive-like and negative bias phenotypes were alleviated after antidepressant administration in both species. In mice, opposite alterations in BLA-to-NAc and BLA-to-CeA neurons activity correlated with this bias (Fig. 5). Furthermore, activation of BLA-to-NAc circuit was sufficient to reverse at least partially the negative emotional bias induced by CORT treatment along with the depressive-like phenotype. Additionally, we showed that CORT treatment induces specific alterations in presynaptic connectivity of BLA projecting neurons. Specifically, CORT-treated mice exhibited less neuronal inputs from the aPVT on BLA-to-NAc neurons but not on BLA-to-CeA neurons, that received more local contacts from BLA neurons.

Emotional bias: a common hallmark in mouse model for depression and depressed patients

We found that chronic CORT treatment induces negative shift of valence assignment on both positive (that became less attractive) and negative (that became more aversive) odors without effect on neutral odor. We observed similar bias in bipolar depression, such that patients rated less odors as pleasant and more odors as unpleasant than both control subjects and remitted patients. Although the low number of control subjects in our study could be a limitation, the fact that this negative bias correlated with

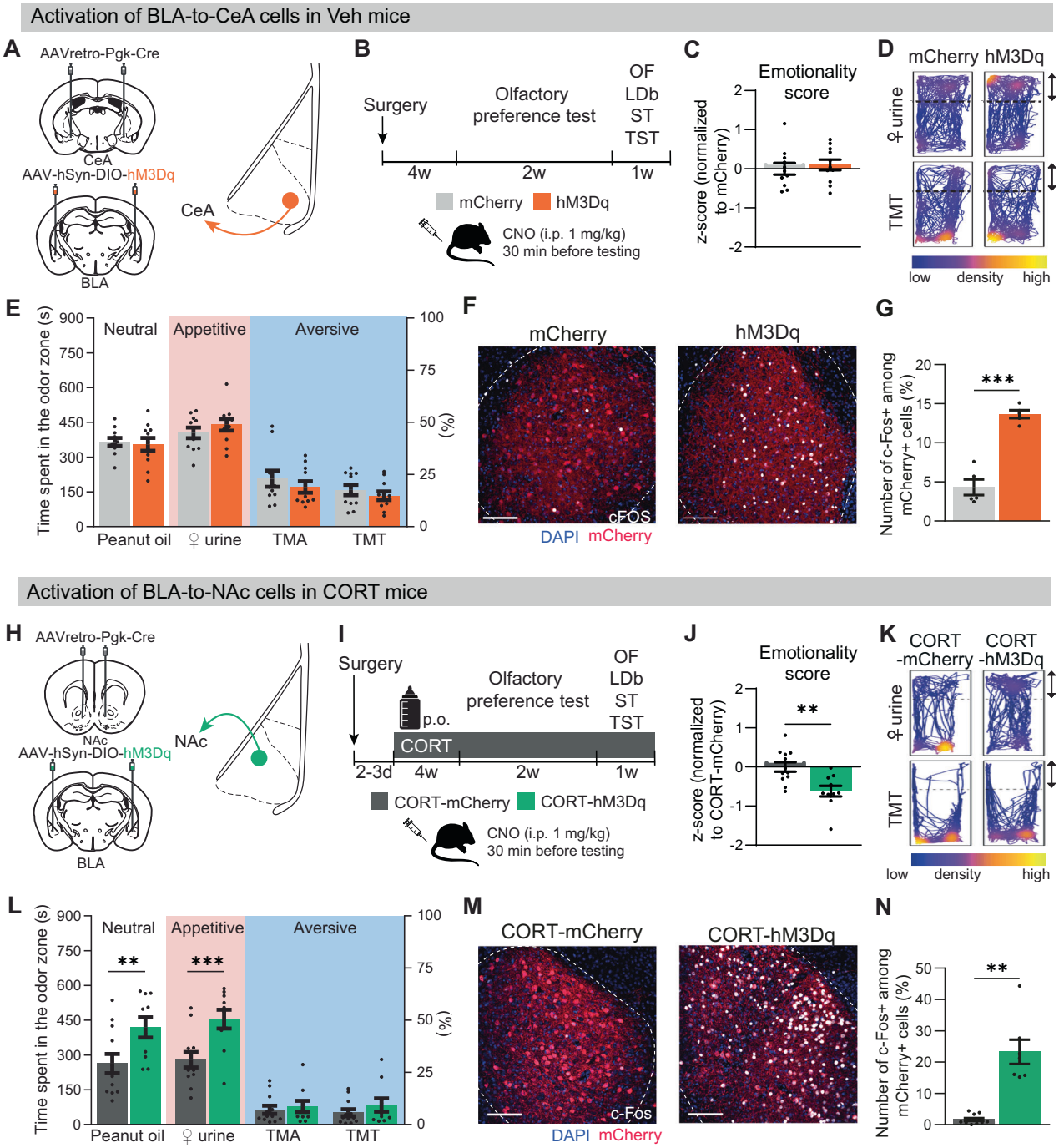

Fig. 4 Chemogenetic activation of BLA circuits distinctly impact CORT phenotype. A To mimic chronic CORT phenotype were injected AAVr-Pgk-Cre in the CeA and AAV-hSyn-DIO-hM3Dq-mCherry (orange, $n = 9$, or AAV-hSyn-DIO-mCherry for the controls, grey, $n = 11$) in the BLA to activate BLA-to-CeA cells (**B**, **C**) CNO intra-peritoneal (i.p.) injection in the hM3Dq mice had no effect on global emotionality score ($t(20) = 0.49$, $p = 0.626$). **D** Representative mouse tracks in the olfactory preference test. **E** Chemogenetic activation of BLA-to-CeA cells did not modify olfactory valence compared to mCherry controls (Group: $F(1,18) = 0.10$, $p = 0.752$; Odor: $F(3,54) = 75.02$, $p < 0.001$; Interaction: $F(3,54) = 1.16$, $p = 0.336$). **F** Representative images of BLA c-Fos expression mCherry (left) and hM3Dq mice (right). **G** Percentage of c-Fos expression among mCherry+ cells after CNO injection (mCherry $n = 5$, hM3Dq $n = 5$; $t(8) = 8.31$, $^{***}p < 0.001$). Total number of mCherry+ cell number analysed dot not diffet between groups ($t(8) = 0.37$, $p = 0.722$). **H** AAVr-Pgk-Cre in the NAc and AAV-hSyn-DIO-hM3Dq-mCherry (green, $n = 10$ or AAV-hSyn-DIO-mCherry for the controls, grey, $n = 12$) in the BLA were injected to activate BLA-to-NAc cells. **I** All mice were treated with CORT. **J** CNO intra-peritoneal (i.p.) injection in the hM3Dq mice reduce the global emotionality score ($t(20) = 3.40$). **K** Representative mouse tracks in the olfactory preference test. **L** CORT-hM3Dq mice explored more peanut oil and ♀ urine relative to CORT-mCherry controls, but not aversive odors (Group: $F(1.20) = 6.56$, $p = 0.019$; Odor: $F(3, 60) = 11.2$, $p < 0.001$; Interaction: $F(3, 60) = 7.31$, $p < 0.001$). **M** Representative images and magnifications of BLA c-Fos expression CORT-mCherry (left) and CORT-hM3Dq mice (right). **N** Percentage of c-Fos expression among mCherry+ cells after CNO injection (CORT-mCherry $n = 12$, CORT-hM3Dq $n = 7$; $t(6.135) = 5.51$). Total number of mCherry+ cell number analysed dot not diffet between groups ($U = 36$, $p = 0.650$). $^{**}p < 0.01$, $^{***}p < 0.001$. Scale bar, 125 µm. Bars are mean ± sem.

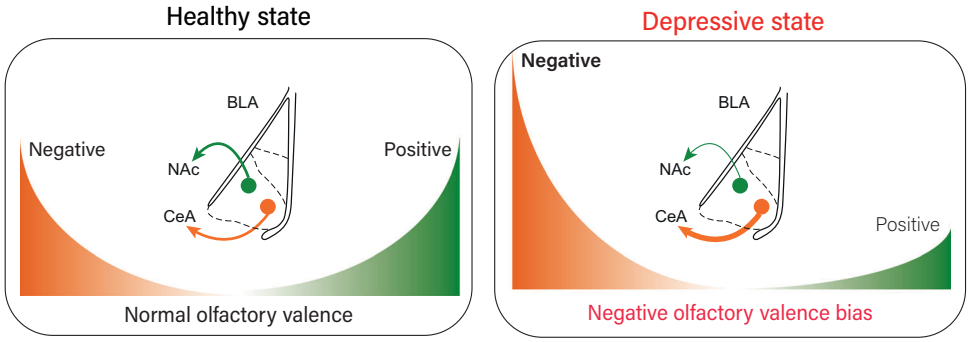

Fig. 5 Summary scheme of the results. Depressive state in both BD patients and CORT-induced model for depression induce a negative olfactory bias (right) respect to healthy state (left). Patients present decreased number of odors rated as pleasant associated with increased number of rated unpleasant odors respect to control subject, while CORT-treated mice exhibit decreased approach behavior towards appetitive odors and increased avoidance behaviour towards aversive odors respect to control group. The chronic CORT administration elevates the activity of BLA projecting neurons to the CeA, which preferentially encode negative valence, and reduces the activity of BLA projecting neurons to the NAc, preferentially encoding positive valence.

depression severity in bipolar patients clearly links mood state with biased valence attribution. Comparably with mice, no difference was found in the valence assignment of neutral odors, suggesting bias specific towards salient emotion-triggering stimuli. Interestingly, this emotional bias regresses after recovery of the depressive episode in patients (i.e. in remitted bipolar patients) and the alleviation of depressive-like phenotype in mice responsive to FLX. These results suggest a major link between depressive states, efficiency of antidepressant drug and the expression of negative emotional bias.

However, extracting the involvement of stimulus intensity processing in our data is still elusive. Indeed, previous results have shown that chronic CORT administration induces deficits in olfactory acuity, fine discrimination of mixed odorants and olfactory memory [31]. In our study, we only analyzed spontaneous responses to individual highly concentrated odors. Furthermore, the increased response to aversive odor in CORT-treated animals reinforces the assumption that mice effectively detected these stimuli.

In human, previous data have shown that emotional bias assessed with olfactory test is present in patients suffering from unipolar depressive episode [44–48]. One study also found modifications in valence assignment in BD depressed patients, but only for pleasant odors [46]. Here, we extend these data, showing that the negative emotional bias affects both positive and negative odors supporting the idea that it represents common hallmark of depressive state, independently of the type of mood disorder.

Our study might be refined by using an animal model specifically designed for bipolar disorders. Nonetheless all facets of bipolar disorders (mania, depression and cyclicity) are currently not reproducible in one and only mice model. Therefore, preclinical studies for bipolar disorders usually only evaluate manic phase [49]. Interestingly, we recently showed by using a multi-dimensional behavioral assessment that the GBR 12909 mice model rather than mimicking mania exhibits a mixed-like state in which both manic and depressive symptoms occur simultaneously, including a strong negative hedonic bias at the opposite of what would be expected from manic mice model [50].

Notably, emotional biases are usually assessed in humans with visual tests such as emotion face recognition or valence assessment of pictures [51]. As not doable in mice, it seemed important to verify that olfactory emotional biases were as relevant in humans as in mice. Consistently, literature on valence coding shows shared neuronal circuits for stimuli from all sensory modalities [52] as well as strong link between olfaction and emotional system throughout evolution [53].

Previous animal behavioral tests exploring valence assignment in BLA circuits mostly involved stimulus association with a reward or aversive punishment outcomes throughout experience or a long learning protocols [7, 8, 18]. To avoid as much as possible any cognitive and motivational confounding factor, we evaluated in mice innate attractive and aversive odor responses such that no previous learning is required, in a more suitable way for an animal model of depression.

Alteration of BLA circuits after CORT administration

To investigate the mechanisms underlying negative bias, we explored circuits involved in valence assignment, particularly BLA circuits. We found that BLA-to-NAc neurons expressed less c-Fos, a proxy for neuronal activity, in CORT-treated animals compared to the Veh-treated control group. Conversely, the density of c-Fos+ BLA-to-CeA neurons was higher in depressed-like mice. Some differences were found in BLA *vs* LA projecting neurons suggesting both regions could be differently affected in depression.

Overall, our data support our hypothesis that specific BLA circuits alterations may support negative bias in a mouse model for depression, in a way that BLA-to-NAc neurons, which preferentially encode positive valence stimuli, are hypoactive during depressive states, whereas BLA-to-CeA preferentially encoding negative valence stimuli are hyperactive ([19–22, 24], but see also [23]). These changes could be due to alterations in the intrinsic electrophysiological properties of different BLA principal neurons and/or modification at the circuit levels. Although our experiments do not allow to untangle the precise mechanism underlying these disruptions, these modifications would promote information flow from BLA to CeA while reducing the output to NAc in depressive states.

Emotional valence coding of environmental cues needs to be dynamic, varying with homeostatic and environmental needs. Our results support the hypothesis that depressive/anxiety states bias stimuli valence processing by propelling BLA network in a negative shifted state that disturb dynamic response to external cues, as previously proposed [5, 54]. Further experiments are required to decipher the time course of these activity dysregulations during depressive-like phenotype instatement and how are they restore by antidepressant treatments.

Chronic stress and increased peripheral cortisol/corticosterone levels might disrupt molecular and cellular neuroplasticity in the BLA affecting both principal neurons and local interneurons. Glucocorticoid receptors are located in all portions of the amygdala [55, 56]. Consistently, chronic stress dramatically impacts BLA principal neurons both at morphological and

physiological levels [36]. Besides the BLA, CORT treatment could affect other brain regions indirectly affecting these circuits [57].

In fact, using rabies virus-based retrograde tracing, we observed modifications of presynaptic inputs to both BLA-to-NAc and BLA-to-CeA neurons following CORT administration. Notably, aPVT, but not pPVT, inputs to BLA-to-NAc neurons were reduced in CORT-treated mice. These results are particularly interesting in regards to recent demonstration of the fundamental role of PVT-to-BLA afferents for valence assignment, controlled through neurotensin (NT) secretion rate [21]. In this study, NT facilitated glutamatergic transmission onto BLA-to-NAc neurons while suppressed it onto BLA-to-CeM. Of note, CORT receptors are also expressed in PVT neurons affecting their function [58]. Our results suggest direct role of the PVT inputs to BLA-to-NAc-projecting neurons in depressive states. Reduced afferents from PVT to BLA-to-NAc neurons could be responsible for their reduced activity rates, disrupting valence assignment of emotional stimuli. Importantly, PVT nucleus has also strong functional connection with the amygdala in human brain [59], and reduction of neurotensin blood levels in human might have a high potential as biomarker to differentiate depressive patients from control subjects [60].

We also found increased inputs contacting BLA-to-CeA neurons from BLA local neurons. The whole BLA is constituted of about 80% of CamkII-expressing glutamatergic pyramidal projection neurons [61], suggesting that higher activity of BLA-to-CeA neurons during depressive states could be due to increased BLA excitatory inputs on these cells. Notably, BLA-to-NAc and BLA-to CeA population neurons mutually control their activity [62, 63]. In this line, a recent study demonstrate that opposing valence-specific ensembles exhibit mutual inhibitory connectivity in vivo [64]. Besides, although less abundant, local interneurons can tightly tune BLA circuits functioning [65].

Of note, the mechanism of trans-synaptic spread of rabies is still not fully understood and could depend on the activity of presynaptic neurons [66–68]. Therefore, in our experiment we cannot decipher if the altered presynaptic connectivity of BLA circuits reported in CORT-treated mice relies on structural and/or functional changes. Further experiments are required to disentangle these alternatives.

Activation of BLA-to-NAc pathway partially restores negative bias

We observed increased activity of BLA-to-CeA neurons in CORT-treated mice suggesting that depressive-like phenotype and negative bias could be mimicked by over-stimulation of this circuit. However, chemogenetically stimulating the BLA-to-CeA pathway in control animals induced neither anxiety- or depressive-like phenotypes, nor a negative olfactory bias. These data confirm that the anxiety/depressive-like phenotype is highly related to emotional bias.

In contrast, activating the BLA-to-NAc circuit reduced the anxiety/depressive-like phenotype in CORT-treated mice and increased attractiveness of both neutral and positive odors. Importantly, BLA-to-NAc neurons are primarily suggested to be involved in reward processing and positive valence assignment, consistently with the effect we observed. However, activating the BLA-to-NAc neurons did not modify the aversion towards negative odors, indicating that other neuronal pathways could be required to restore the bias regarding aversive odors. Negative stimuli predicting danger might rely on multiple evolutionally selected and redundant mechanisms more difficult to hijack.

Interestingly, CNO administration induce the activation of only 15% ~ 25% of hM3Dq-mCherry+ cells, which could be explained by the low dose choose to avoid confounding anxiolytic/antipsychotic, as already described [69, 70]. In addition, the restricted activation obtain in BLA neurons might be consequence of circuit-dependent regulations of their neuronal activity. For instance, BLA-to-CeA neurons in control mice as well as BLA-to-NAc in CORT-treated mice might be submitted to over-inhibition at baseline.

Our gain-of-function approach reveals of the role of BLA circuits on valence assignment bias and depressive symptoms, but inhibition of these circuits, in particular BLA-to-CeA neurons in CORT-treated mice, might be essential to investigate their involvement in these phenotypes.

Importantly, the present data agree with the observed neural changes in BLA circuits and demonstrate that activation of BLA-to-NAc projecting neurons is able to improve positive valence assignment, providing a mechanism to alleviate anxiety/depressive-like phenotype in CORT-treated mice [71]. Interestingly, this neuronal activity manipulation mimicked the action of FLX in responsive mice. Together with previous studies [24, 72, 73], our results suggest BLA-to-NAc neurons might represent a common pathway for antidepressant action and a potential therapeutic target for future drug development.

In summary, we show for the first time a negative bias in valence assignment in a mouse model for depression recapitulating the emotional bias found in depressed patients. This bias is related to plasticity in BLA circuits known to be involved in valence assignment. Futures steps will require to explore the effect of various classes of antidepressants on negative emotional bias and BLA circuits activity. Identifying a common behavioral and neuronal mechanism of action for different antidepressant should be of great help for improving therapeutic management of depression. If reversibility of emotional negative bias is mandatory to expect antidepressant action, new molecules should be assessed in pre-clinical studies using olfactory valence evaluation, complementing the gold standard but challenged forced swim and tail suspension tests [74]. As recently emphasized [16], reliable dimensional phenotypes, including both positive and negative emotional evaluation, and the development of integrative cross-species models will be crucial to disentangle the psychopathology of depression and ultimately contribute to alleviate suffering patients.

DATA AVAILABILITY

The datasets and codes that support the findings of this study are available from the corresponding author upon reasonable request.

CODE AVAILABILITY

The datasets and codes that support the findings of this study are available from the corresponding author upon reasonable request.

REFERENCES

1. Global, regional, and national burden of 12 mental disorders in 204 countries and territories, 1990–2019: a systematic analysis for the Global Burden of Disease Study 2019. The Lancet Psychiatry 2022;9:137–50.
2. Leppänen JM. Emotional information processing in mood disorders: a review of behavioral and neuroimaging findings. Curr Opin Psychiatry. 2006;19:34–9.
3. Clark L, Chamberlain SR, Sahakian BJ. Neurocognitive Mechanisms in Depression: Implications for Treatment. Annu Rev Neurosci. 2009;32:57–74.
4. Harmer CJ, O'Sullivan U, Favaron E, Massey-Chase R, Ayres R, Reinecke A, et al. Effect of Acute Antidepressant Administration on Negative Affective Bias in Depressed Patients. AJP. 2009;166:1178–84.
5. Bigot M, Alonso M, Houenou J, Sarrazin S, Dargél AA, Lledo P-M, et al. An emotional-response model of bipolar disorders integrating recent findings on amygdala circuits. Neurosci Biobehav Rev. 2020;118:358–66.
6. Beck AT, Bredemeier K. A Unified Model of Depression: Integrating Clinical, Cognitive, Biological, and Evolutionary Perspectives. Clin Psychological Sci. 2016;4:596–619.
7. Hales CA, Stuart SA, Anderson MH, Robinson ESJ. Modelling cognitive affective biases in major depressive disorder using rodents. Br J Pharm. 2014;171:4524–38.
8. Hinchcliffe JK, Stuart SA, Mendl M, Robinson ESJ. Further validation of the affective bias test for predicting antidepressant and pro-depressant risk: effects of pharmacological and social manipulations in male and female rats [no. 20]. Psychopharmacology. 2017;234:3105–16.

9. Phillips ML, Ladouceur CD, Drevets WC. A neural model of voluntary and automatic emotion regulation: implications for understanding the pathophysiology and neurodevelopment of bipolar disorder. Mol Psychiatry. 2008;13:833–57.
10. Groenewold NA, Opmeer EM, De Jonge P, Aleman A, Costafreda SG. Emotional valence modulates brain functional abnormalities in depression: Evidence from a meta-analysis of fMRI studies. Neurosci Biobehav Rev. 2013;37:152–63.
11. Liu H, Wang C, Lan X, Li W, Zhang F, Fu L, et al. Functional connectivity of the amygdala and the antidepressant and antisuicidal effects of repeated ketamine infusions in major depressive disorder. Front Neurosci. 2023;17:1123797.
12. Wen X, Han B, Li H, Dou F, Wei G, Hou G, et al. Unbalanced amygdala communication in major depressive disorder. J Affect Disord. 2023;329:192–206.
13. Bellani M, Baiano M, Brambilla P. Brain anatomy of major depression II. Focus on amygdala. Epidemiol Psychiatr Sci. 2011;20:33–6.
14. Gaffrey MS, Luby JL, Belden AC, Hirshberg JS, Volsch J, Barch DM. Association between depression severity and amygdala reactivity during sad face viewing in depressed preschoolers: an fMRI study. J Affect Disord. 2011;129:364–70.
15. Godlewska BR, Norbury R, Selvaraj S, Cowen PJ, Harmer CJ. Short-term SSRI treatment normalises amygdala hyperactivity in depressed patients. Psychol Med. 2012;42:2609–17.
16. Grogans SE, Fox AS, Shackman AJ. The Amygdala and Depression: A Sober Reconsideration. AJP. 2022;179:454–7.
17. Fox AS, Oler JA, Tromp DPM, Fudge JL, Kalin NH. Extending the amygdala in theories of threat processing. Trends Neurosci. 2015;38:319–29.
18. Pignatelli M, Beyeler A. Valence coding in amygdala circuits. Curr Opin Behav Sci. 2019;26:97–106.
19. Namburi P, Beyeler A, Yorozu S, Calhoon GG, Halbert SA, Wichmann R, et al. A circuit mechanism for differentiating positive and negative associations. Nature. 2015;520:675–8.
20. Beyeler A, Namburi P, Glober GF, Simonnet C, Calhoon GG, Conyers GF, et al. Divergent Routing of Positive and Negative Information from the Amygdala during Memory Retrieval. Neuron. 2016;90:348–61.
21. Li H, Namburi P, Olson JM, Borio M, Lemieux ME, Beyeler A, et al. Neurotensin orchestrates valence assignment in the amygdala. Nature. 2022;608:586–92.
22. Zhang X, Guan W, Yang T, Furlan A, Xiao X, Yu K, et al. Genetically identified amygdala–striatal circuits for valence-specific behaviors. Nat Neurosci. 2021;24:1586–1600.
23. Shen C-J, Zheng D, Li K-X, Yang J-M, Pan H-Q, Yu X-D, et al. Cannabinoid CB1 receptors in the amygdalar cholecystokinin glutamatergic afferents to nucleus accumbens modulate depressive-like behavior. Nat Med. 2019 https://doi.org/10.1038/s41591-018-0299-9.
24. Zhou K, Xu H, Lu S, Jiang S, Hou G, Deng X, et al. Reward and aversion processing by input-defined parallel nucleus accumbens circuits in mice [no. 1]. Nat Commun. 2022;13:6244.
25. American Psychiatric Association (2000): *DSM-IV-TR: Diagnostic and Statistical Manual of Mental Disorders*.
26. Swiecicki L, Zatorski P, Bzinkowska D, Sienkiewicz-Jarosz H, Szyndler J, Scinska A. Gustatory and olfactory function in patients with unipolar and bipolar depression. Prog Neuro-Psychopharmacol Biol Psychiatry. 2009;33:827–34.
27. David DJ, Samuels BA, Rainer Q, Wang J-W, Marsteller D, Mendez I, et al. Neurogenesis-Dependent and -Independent Effects of Fluoxetine in an Animal Model of Anxiety/Depression. Neuron. 2009;62:479–93.
28. Pérez-Gómez A, Bleymehl K, Stein B, Pyrski M, Birnbaumer L, Munger SD, et al. Innate Predator Odor Aversion Driven by Parallel Olfactory Subsystems that Converge in the Ventromedial Hypothalamus. Curr Biol. 2015;25:1340–6.
29. Hummel T, Kobal G, Gudziol H, Mackay-Sim A. Normative data for the "Sniffin' Sticks" including tests of odor identification, odor discrimination, and olfactory thresholds: an upgrade based on a group of more than 3000 subjects. Eur Arch Otorhinolaryngol. 2007;264:237–43.
30. Rumeau C, Nguyen DT, Jankowski R. How to assess olfactory performance with the Sniffin'Sticks test®. Eur Ann Otorhinolaryngol Head Neck Dis. 2016;133:203–6.
31. Siopi E, Denizet M, Gabellec M-M, de Chaumont F, Olivo-Marin J-C, Guilloux J-P, et al. Anxiety- and Depression-Like States Lead to Pronounced Olfactory Deficits and Impaired Adult Neurogenesis in Mice. J Neurosci. 2016;36:518–31.
32. Mendez-David I, Boursier C, Domergue V, Colle R, Falissard B, Corruble E, et al. Differential Peripheral Proteomic Biosignature of Fluoxetine Response in a Mouse Model of Anxiety/Depression. Front Cell Neurosci. 2017;11:237.
33. Nierenberg AA, DeCecco LM. Definitions of antidepressant treatment response, remission, nonresponse, partial response, and other relevant outcomes: a focus on treatment-resistant depression. J Clin Psychiatry. 2001;62:5–9.
34. Grelat A, Benoit L, Wagner S, Moigneu C, Lledo P-M, Alonso M. Adult-born neurons boost odor-reward association. Proc Natl Acad Sci USA 2018;115:2514–9.
35. Gothard KM. Multidimensional processing in the amygdala. Nat Rev Neurosci. 2020;21:565–75.
36. Roozendaal B, McEwen BS, Chattarji S. Stress, memory and the amygdala. Nat Rev Neurosci. 2009;10:423–33.
37. The Amygdaloid Complex: Anatomy and Physiology (n.d.): https://doi.org/10.1152/physrev.00002.2003.
38. Kim J, Pignatelli M, Xu S, Itohara S, Tonegawa S. Antagonistic negative and positive neurons of the basolateral amygdala. Nat Neurosci. 2016;19:1636–46.
39. Zhang W-H, Zhang J-Y, Holmes A, Pan B-X. Amygdala Circuit Substrates for Stress Adaptation and Adversity. Biol Psychiatry. 2021;89:847–56.
40. Morikawa S, Katori K, Takeuchi H, Ikegaya Y. Brain-wide mapping of presynaptic inputs to basolateral amygdala neurons. J Compar Neurol. 2021;529:3062–75.
41. Hintiryan H, Bowman I, Johnson DL, Korobkova L, Zhu M, Khanjani N, et al. Connectivity characterization of the mouse basolateral amygdalar complex. Nat Commun. 2021;12:1–25.
42. Gao C, Leng Y, Ma J, Rooke V, Rodriguez-Gonzalez S, Ramakrishnan C, et al. Two genetically, anatomically and functionally distinct cell types segregate across anteroposterior axis of paraventricular thalamus. Nat Neurosci. 2020;23:217–28.
43. Kirouac GJ. Placing the paraventricular nucleus of the thalamus within the brain circuits that control behavior. Neurosci Biobehav Rev. 2015;56:315–29.
44. Colle R, El Asmar K, Verstuyft C, Lledo P-M, Lazarini F, Chappell K, et al. The olfactory deficits of depressed patients are restored after remission with venlafaxine treatment. Psychol Med. 2020;22:1–9.
45. Kohli P, Soler ZM, Nguyen SA, Muus JS, Schlosser RJ. The Association Between Olfaction and Depression: A Systematic Review. Chem Senses. 2016;41:479–86.
46. Kazour F, Richa S, Char CA, Surget A, Elhage W, Atanasova B. Olfactory markers for depression: Differences between bipolar and unipolar patients. PLOS ONE. 2020;15:e0237565.
47. Atanasova B, El-Hage W, Chabanet C, Gaillard P, Belzung C, Camus V. Olfactory anhedonia and negative olfactory alliesthesia in depressed patients. Psychiatry Res. 2010;176:190–6.
48. Naudin M, El-Hage W, Gomes M, Gaillard P, Belzung C, Atanasova B. State and Trait Olfactory Markers of Major Depression. PLOS ONE. 2012;7:e46938.
49. Cosgrove VE, Kelsoe JR, Suppes T. Toward a Valid Animal Model of Bipolar Disorder: How the Research Domain Criteria Help Bridge the Clinical-Basic Science Divide [no. 1]. Biol Psychiatry. 2016;79:62–70.
50. Bigot M, Vicq E, Lledo P-M, Alonso M, Henry C. Assessing positive and negative valence systems to refine animal models of bipolar disorders: the example of GBR 12909-induced manic phenotype. Sci Rep. 2022;12:7364.
51. Feng C, Gu R, Li T, Wang L, Zhang Z, Luo W, et al. Separate neural networks of implicit emotional processing between pictures and words: A coordinate-based meta-analysis of brain imaging studies. Neurosci Biobehav Rev. 2021;131:331–44.
52. Richardson JS. The amygdala: historical and functional analysis. Acta Neurobiol Exp. 1973;33:623–48.
53. Kontaris I, East BS, Wilson DA. Behavioral and Neurobiological Convergence of Odor, Mood and Emotion: A Review. Front Behav Neurosci. 2020;14:35.
54. Antonoudiou P, Stone B, Colmers PLW, Evans-Strong A, Walton N, Maguire J. Influence of chronic stress on network states governing valence processing: Potential relevance to the risk for psychiatric illnesses. J Neuroendocrinol. 2023;35:e13274.
55. Hartmann J, Dedic N, Pöhlmann ML, Häusl A, Karst H, Engelhardt C, et al. Forebrain glutamatergic, but not GABAergic, neurons mediate anxiogenic effects of the glucocorticoid receptor. Mol Psychiatry. 2017;22:466–75.
56. Kolber BJ, Roberts MS, Howell MP, Wozniak DF, Sands MS, Muglia LJ. Central amygdala glucocorticoid receptor action promotes fear-associated CRH activation and conditioning. PNAS. 2008;105:12004–9.
57. McEwen BS, Akil H. Revisiting the Stress Concept: Implications for Affective Disorders. J Neurosci. 2020;40:12–21.
58. Jaferi A, Bhatnagar S. Corticosterone can act at the posterior paraventricular thalamus to inhibit hypothalamic-pituitary-adrenal activity in animals that habituate to repeated stress. Endocrinology. 2006;147:4917–30.
59. Kark SM, Birnie MT, Baram TZ, Yassa MA. Functional Connectivity of the Human Paraventricular Thalamic Nucleus: Insights From High Field Functional MRI. Front Integr Neurosci. 2021;15:662293.
60. Yu H, Ni P, Zhao L, Tian Y, Li M, Li X, et al. Decreased plasma neuropeptides in first-episode schizophrenia, bipolar disorder, major depressive disorder: associations with clinical symptoms and cognitive function. Front Psychiatry. 2023;14:1180720.
61. McDonald AJ. Functional neuroanatomy of the basolateral amygdala: Neurons, neurotransmitters, and circuits. Handb Behav Neurosci. 2020;26:1–38.
62. Beyeler A, Chang C-J, Silvestre M, Lévêque C, Namburi P, Wildes CP, et al. Organization of Valence-Encoding and Projection-Defined Neurons in the Basolateral Amygdala. Cell Rep. 2018;22:905–18.
63. Calhoon GG, Sutton AK, Chang C-J, Libster AM, Glober GF, Lévêque CL, et al. Acute Food Deprivation Rapidly Modifies Valence-Coding Microcircuits in the Amygdala. *bioRxiv* 285189. 2018.
64. Piantadosi SC, Zhou ZC, Pizzano C, Pedersen CE, Nguyen TK, Thai S, et al. Holographic stimulation of opposing amygdala ensembles bidirectionally modulates valence-specific behavior via mutual inhibition. Neuron. 2024;112:593–610.e5.

65. Prager EM, Bergstrom HC, Wynn GH, Braga MFM. The basolateral amygdala γ-aminobutyric acidergic system in health and disease: BLA GABAergic System in Health and Disease. J Neurosci Res. 2016;94:548–67.
66. Saleeba C, Dempsey B, Le S, Goodchild A, McMullan S. A Student's Guide to Neural Circuit Tracing. Front Neurosci. 2019;13:897.
67. Rogers A, Beier KT. Can transsynaptic viral strategies be used to reveal functional aspects of neural circuitry? J Neurosci Methods. 2021;348:109005.
68. Ugolini G. Viruses in connectomics: Viral transneuronal tracers and genetically modified recombinants as neuroscience research tools. J Neurosci Methods. 2020;346:108917.
69. MacLaren DAA, Browne RW, Shaw JK, Krishnan Radhakrishnan S, Khare P, España RA, et al. Clozapine N-Oxide Administration Produces Behavioral Effects in Long-Evans Rats: Implications for Designing DREADD Experiments. eNeuro. 2016;3:ENEURO.0219–16.2016.
70. Mahler SV, Aston-Jones G. CNO Evil? Considerations for the Use of DREADDs in Behavioral Neuroscience. Neuropsychopharmacology. 2018;43:934–6.
71. Harmer CJ, Duman RS, Cowen PJ. How do antidepressants work? New perspectives for refining future treatment approaches. Lancet Psychiatry. 2017;4:409–18.
72. Ramirez S, Liu X, MacDonald CJ, Moffa A, Zhou J, Redondo RL, et al. Activating positive memory engrams suppresses depression-like behaviour. Nature. 2015;522:335–9.
73. Dieterich A, Floeder J, Stech K, Lee J, Srivastava P, Barker DJ, et al. Activation of Basolateral Amygdala to Nucleus Accumbens Projection Neurons Attenuates Chronic Corticosterone-Induced Behavioral Deficits in Male Mice. Front Behav Neurosci. 2021;15:643272.
74. Reardon S. Depression researchers rethink popular mouse swim tests. Nature. 2019;571:456–7.

ACKNOWLEDGEMENTS

We thank Denis David for advices on the corticosterone-induced model for depression, the Institut Pasteur Central animal facility and especially Noémi Dominique for her assistance with behavioral experiments, Corentin Guérinot for his advices in the PCA analyses and the Institut Pasteur Image analysis hub for help in developing the Icy protocol. We thank G Lepousez, A Nissant, K Sailor for critical reading of the manuscript and all Perception and Action lab members their constructive inputs. This work was supported by Agence Nationale de la Recherche Grants ANR-15-NEUC-0004-02 "Circuit-OPL", Laboratory for Excellence Programme "Revive" Grant ANR-10-LABX-73, ANR-AAPG2021 "EMOKET", the Life Insurance Company AG2R-La Mondiale, Labex BioPsy and the Fondation Deniker.

AUTHOR CONTRIBUTIONS

MB: Conceptualization, Methodology, Investigation, Formal analysis, Visualization, Writing – Original Draft, Writing – Review and Editing; CHDB, AB, EV, MM: Investigation, Formal analysis, Visualization; SW, AAH: Tool development; PML, JH: Writing – Review and Editing, Supervision, Funding acquisition; CH: Conceptualization, Methodology, Writing – Original Draft, Writing – Review and Editing, Supervision, Funding acquisition. MA: Conceptualization, Methodology, Investigation, Formal analysis, Visualization, Writing – Original Draft, Writing – Review and Editing, Supervision, Funding acquisition.

COMPETING INTERESTS

The authors declare no competing interests.

ADDITIONAL INFORMATION

Supplementary information The online version contains supplementary material available at https://doi.org/10.1038/s41398-024-03085-6.

Correspondence and requests for materials should be addressed to Chantal Henry or Mariana Alonso.